

Supplementary information for:

Donor-Acceptor Organo-Imido Polyoxometalates: High Transparency, High Activity Redox-Active NLO Chromophores

Ahmed Al-Yasari, Nick Van Steerteghem, Hani El Moll, Koen Clays and John Fielden.

General

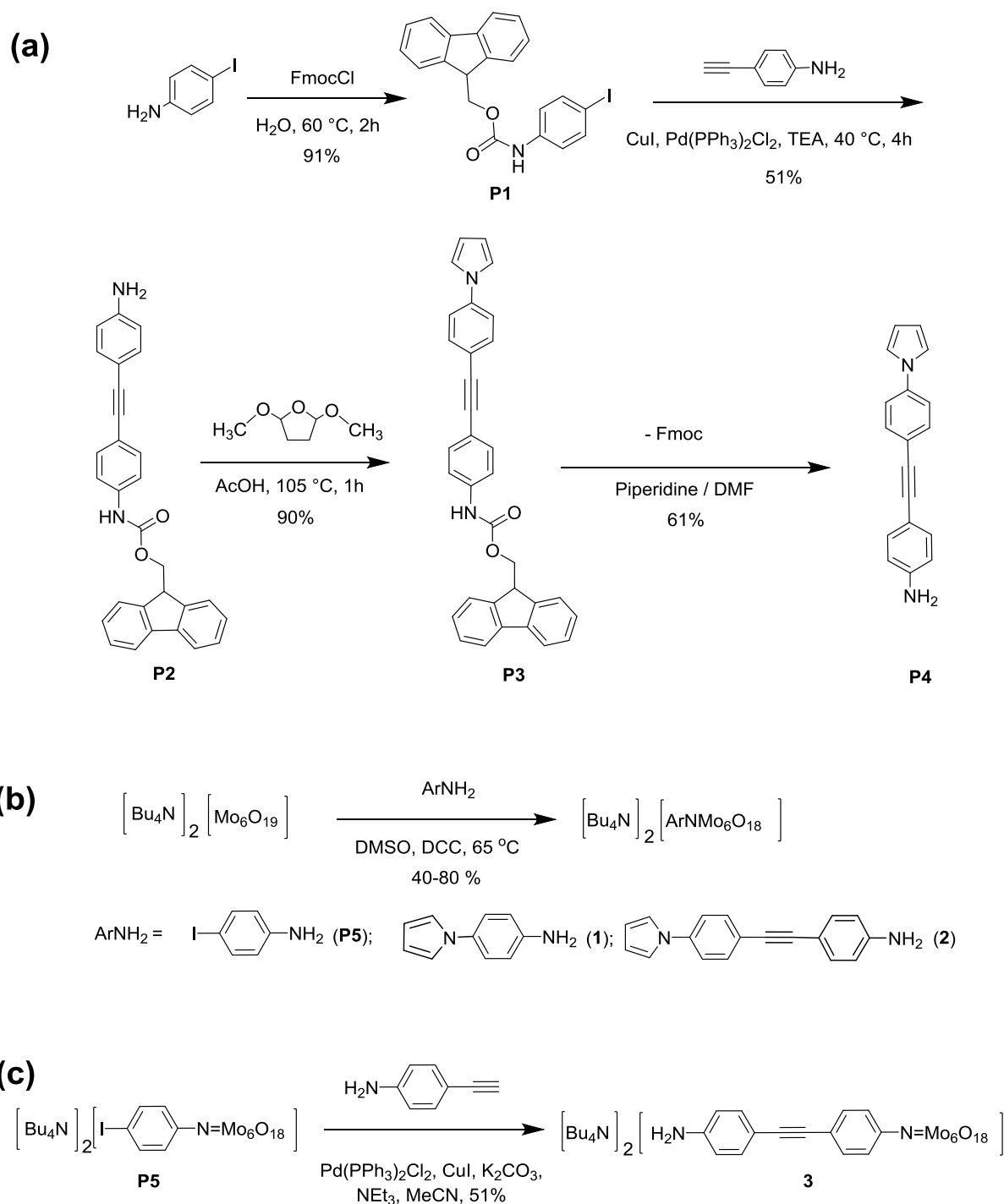
Materials and Procedures. Tetrahydrofuran (THF), acetonitrile (MeCN) and dimethylformamide (DMF) were freshly distilled under nitrogen from an appropriate drying agent.¹ Dry (sure seal) dimethyl sulfoxide (DMSO) was purchased from Sigma Aldrich. All other reagents and solvents were obtained as ACS grade from Sigma Aldrich, Alfa Aesar or Fisher Scientific and used as supplied. The compounds tetrabutylammonium hexamolybdate,² and 4-(1H-pyrrol-1-yl)aniline³ were synthesized according to previously published methods. 4-{[4-(1H-pyrrol-1-yl)phenyl]ethynyl}aniline was following synthetic route shown in Scheme S1. Organoimido hexamolybdate derivatives were synthesised using an adapted literature procedure,⁴ under an atmosphere of dry nitrogen using standard schlenk techniques.

Physical Measurements. FT-IR spectra were measured using Perkin Elmer FT-IR spectrum BX and Bruker FT-IR XSA spectrometers. ¹H- and ¹³C-NMR spectra were acquired using Bruker AC 300 (300 MHz) and Bruker Ascend 500 (500 MHz) spectrometers and all shifts are quoted with respect to TMS using the solvent signals as secondary standard (s = singlet, d = doublet, t = triplet, q = quartet, sex = sextet, dt = doublet of triplets, m = multiplet). Quaternary carbon signals were not observed for these compounds even after 1064 scans of saturated d₆-DMSO solutions, which gave strong signal for all other ¹³C resonances. Elemental analyses and accurate mass spectrometry were outsourced to London Metropolitan University, and the UK National Mass Spectrometry Service at Swansea University respectively. UV-Vis spectra were obtained by using an Agilent Cary 60 UV-Vis spectrophotometer. Cyclic voltammetric measurements were carried out using Autolab PGStat 30 potentiostat/galvanostat. A single-compartment or a conventional three-electrode cell was used with a silver/silver chloride reference electrode (3M NaCl, saturated AgCl), glassy carbon or platinum working electrode and Pt wire auxiliary electrode. Acetonitrile was freshly distilled (from CaH₂), [N(C₄H₉-n)₄]PF₆, as supplied from Fluka, and [N(C₄H₉-n)₄]BF₄,⁵ were used as the supporting electrolyte. Solutions containing ca. 10⁻³ M analyte (0.1 M electrolyte) were degassed by purging with nitrogen. All *E*_{1/2} values were calculated from (*E*_{pa} + *E*_{pc})/2 at a scan rate of 100 mV s⁻¹ and referenced to Fc/Fc⁺.

Synthetic Methods

Summary. Our synthetic approach is summarized in Scheme S1. Hexamolybdate derivatives were obtained through DCC-mediated coupling of anilines with hexamolybdate, using an excess (1.3 equivalents) of [NBu₄]₂[Mo₆O₁₉] to prevent formation of *bis*-imido products. The precursor 4-{[4-(1H-pyrrol-1-yl)phenyl]ethynyl}aniline (**P4**) was obtained through a multistep synthesis using an Fmoc protection strategy, and [NBu₄]₂[**3**] by post-functionalization of arylido derivatized hexamolybdate **P5** by Sonogashira coupling.⁶ Attempts to obtain [NBu₄]₂[**2**] through Sonogashira post-functionalization failed due to side-reactions involving the pyrrole group, while DCC-coupling of dianilines with [Mo₆O₁₉]²⁻ (e.g. the alternative route to [NBu₄]₂[**3**]) produce mixtures of *mono*- and *bis*-Lindqvist products which are very difficult to separate. Note that while all of the compounds show evidence of [Mo₆O₁₉]²⁻ in the ESI-MS, this must result from fragmentation: elemental analyses are an excellent fit for the targets, ¹H-NMR integration showed no evidence of “excess”

tetrabutylammonium cations that would accompany $[\text{Mo}_6\text{O}_{19}]^{2-}$, and cyclic voltammetry of the final products did not show evidence of the $[\text{Mo}_6\text{O}_{19}]^{2-/3-}$ couple (reversible wave at $E_{1/2} = -0.315 \text{ V vs Ag/AgCl}$).



Scheme S1 Synthetic approach to precursors and hexamolybdate derivatives. **(a)** Synthesis of 4-{[4-(1H-pyrrol-1-yl)phenyl]ethynyl}aniline (**P4**). **(b)** DCC-mediated synthesis of hexamolybdate derivatives. **(c)** Sonogashira post-functionalization used to access $[\text{NBu}_4]_2[\mathbf{3}]$.

Synthesis of 9H-fluoren-9-ylmethyl (4-iodophenyl)carbamate (P1). The procedure to prepare **P1** was based on the method of Gawande and Branco.⁷ N-(9-fluorenylmethoxycarbonyl) chloride (FmocCl) (0.310 g, 1.2 mmol), 4-iodoaniline (0.219 g, 1 mmol) and 3 mL H₂O were heated at 60 °C for 2 hours. The reaction was monitored by thin layer chromatography using ethyl acetate:hexane (3:7) as eluent. The crude product was filtered and washed with water and then recrystallized from hot ethanol to yield the pure product (0.4 g, 0.906 mmol, 91 %). δ_{H} (500 MHz, (CD₃)₂SO) 9.82 (s, 1H), 7.91 (d, $J = 7.5$ Hz, 2H), 7.74 (d, $J = 7.5$ Hz, 2H), 7.59 (d, $J = 7.9$ Hz, 2H), 7.42 (t, $J = 7.5$ Hz, 2H), 7.35 (t, $J = 7.5$ Hz, 2H), 7.30 (s, 2H), 4.50 (d, $J = 6.2$ Hz, 2H), 4.31 (t, $J = 6.2$ Hz, 1H). δ_{C} (125 MHz, (CD₃)₂SO) 153.28, 143.72, 140.82, 138.90, 137.34, 127.71, 127.14, 125.10, 120.49, 120.20, 85.74, 65.66, 46.59. Anal. Calcd (found) % for C₂₁H₁₆INO₂: C, 57.15 (57.21); H, 3.65 (3.54); N, 3.17 (3.29). $m/z = 442$ [C₂₁H₁₆INO₂H]⁺. FTIR: 3342 (w); 1739 (s); 1586 (m); 1526 (s); 1446 (w); 1396 (m); 1309 (m); 1287 (w); 1237 (m); 1221 (s); 1104 (m); 1089 (m); 1063 (w); 1048 (m); 1003 (m); 986 (w); 935 (vw); 817 (s); 763 (m); 736 (vs); 621 (m); 547 (m).

Synthesis of N-(9-Fluorenylmethoxycarbonyl)-4-[(4-iodophenyl)ethynyl]aniline (P2). **P1** (2.206 g, 5 mmol), 4-ethynylaniline (1.16 g, 5.3 mmol), Pd(PPh₃)₂Cl₂ (3 mol%, 0.111 g, 0.159 mmol), and CuI (5 mol%, 0.05 g, 0.265 mmol) were added to an oven-dried 50 mL two neck flask. Anhydrous THF (25 mL) and dry triethylamine (2 mL) were then added to the flask and the reaction mixture was stirred at 40 °C under nitrogen. The reaction was monitored by thin layer chromatography using ethyl acetate 8:2 toluene. After consumption of the amine (4 hours), the product was filtered, 50 mL H₂O added, and extracted twice with DCM (2 × 30 mL). The combined organic layers were washed with H₂O (2 × 60 mL) before being dried over anhydrous MgSO₄. The solution was then diluted with DCM and layered with hexane. The red precipitate was filtered off and the filtrate was concentrated in rotary evaporator to afford the crude product. This was re-dissolved in the minimum DCM and layered with hexane to give a brown solid (1.1 g, 2.55 mmol, 51 %). δ_{H} (500 MHz, (CD₃)₂CO) 9.01 (s, 1H), 7.88 (d, $J = 7.5$ Hz, 2H), 7.73 (d, $J = 7.5$ Hz, 2H), 7.56 (s, 2H), 7.45-7.32 (m, 6H), 7.23 (d, $J = 8.8$ Hz, 2H), 6.67 (d, $J = 8.8$ Hz, 2H), 5.02 (s, 2H), 4.52 (d, $J = 6.6$ Hz, 2H), 4.31 (t, $J = 6.6$ Hz, 1H). δ_{C} (125 MHz, (CD₃)₂CO) 154.27, 149.91, 145.03, 142.24, 139.74, 138.63, 133.46, 132.61, 128.67, 128.05, 126.07, 120.95, 119.10, 114.95, 111.44, 90.68, 87.31, 67.17, 48.00. Anal. Calcd (found) % for C₂₉H₂₂N₂O₂: C, 80.90 (80.78); H, 5.15 (5.22); N, 6.50 (6.49). $m/z = 431.17$ [C₂₉H₂₂N₂O₂H]⁺. FTIR: 3343 (w); 1706 (s); 1607 (m); 1581 (m); 1521 (vs); 1449 (w); 1407 (m); 1309 (m); 1219 (vs); 1137 (w); 1104 (m); 1087 (m); 1050 (s); 982 (vw); 830 (vs); 736 (vs); 644 (m); 620 (m).

Synthesis of N-(9-Fluorenylmethoxycarbonyl)-4-[4-(phenylethynyl)phenyl]-1H-pyrrole (P3). **P3** was synthesized according to the Clauson-Kaas method.⁸ A mixture of **P2** (0.430 g, 1 mmol), 2,5-dimethoxytetrahydrofuran (0.145 g, 1.1 mmol), and 10 mL acetic acid were added to an oven-dried 50 mL round bottom flask containing a magnetic stir bar. The reaction mixture was reflux for 1 hour under nitrogen and monitored by thin layer chromatography using ethyl acetate 9:1 toluene. After cooling to room temperature 20 mL H₂O was added and the resulting solution was extracted with DCM (3 × 15 mL). The DCM phase was washed with H₂O (2 × 100 mL) before being dried over anhydrous MgSO₄. The solution was then reduced to dryness under vacuum to give a red solid (0.43 g, 0.89 mmol, 89 %). δ_{H} (500 MHz, CDCl₃) 7.80 (d, $J = 7.4$ Hz, 2H), 7.64 (d, $J = 7.7$ Hz, 2H), 7.58 (d, $J = 8.7$ Hz, 2H), 7.51-7.31 (m, 10H), 7.12 (t, $J = 2.5$ Hz, 2H), 6.71 (s, 1H), 6.38 (t, $J = 2.5$ Hz, 2H), 4.59 (d, $J = 6.4$ Hz, 2H), 4.30 (t, $J = 6.4$ Hz, 1H). δ_{C} (125 MHz, CDCl₃) 143.62, 141.39, 140.14, 132.78, 132.43, 127.84, 127.15, 124.84, 120.48, 120.11, 119.99, 119.07, 118.34, 118.07, 110.91, 101.43, 89.54, 88.16, 66.99, 47.06, 38.76. $m/z = 481$ [C₃₃H₂₄N₂O₂H]⁺. Note that **P3**, like many pyrroles, undergoes oxidation very easily upon exposure to air or acid conditions. For this reason we were unable to chromatographically purify the material or obtain satisfactory elemental analysis. The

crude material was directly reacted on to make **P4** (see below), which is more stable and gave a good elemental analysis result.

Synthesis of 4-[[4-(1H-pyrrol-1-yl)phenyl]ethynyl]aniline (P4). To a solution of **P3** (0.427 g, 0.89 mmol) in 10 mL anhydrous DMF, 5 mL piperidine was added before stirring for 30 minutes under nitrogen. The mixture was then layered with 20 mL H₂O to give a creamy brown precipitate before being filtered and dried. The brown solid was dissolved in 50 mL acetone and then layered with H₂O to give brown precipitate of cleaved Fmoc by product. This was filtered off and the filtrate was layered with H₂O to give a yellow solid which was then washed with H₂O and dried in air before being dissolved in diethyl ether. The diethyl ether phase was dried over anhydrous MgSO₄, filtered and evaporated to dryness under vacuum to afford a yellow solid (0.14 g, 0.54 mmol, 61 %). δ_{H} (300 MHz, CDCl₃) 7.55 (d, $J = 8.8$ Hz, 2H), 7.37 (d, $J = 3.1$ Hz, 2H), 7.35 (d, $J = 3.1$ Hz, 2H), 7.12 (t, $J = 2.2$ Hz, 2H), 6.66 (d, $J = 8.8$ Hz, 2H), 6.37 (t, $J = 2.2$ Hz, 2H), 3.84 (s, 2H). δ_{C} (125 MHz, CDCl₃) 146.70, 139.77, 132.95, 132.57, 121.10, 120.00, 119.03, 114.76, 112.48, 110.76, 90.57, 86.62. Anal. Calcd (found) % for C₂₉H₂₂N₂O₂: C, 83.68 (83.61); H, 5.46 (5.38); N, 10.85 (11.00). $m/z = 259$ ([C₁₈H₁₄N₂H]⁺). FTIR: 3425 (w); 3332 (sh); 3215(w); 2213 (vw); 1605 (s); 1523 (m); 1476 (m); 1323 (s); 1279 (m); 1120 (m); 1070 (m); 1016 (m); 918 (m); 827 (vs); 725 (vs); 613 (s). UV-Vis (MeCN) λ , nm (ϵ , M⁻¹ cm⁻¹): 320 (44.7×10³).

Synthesis of [(C₄H₉)₄N]₂[Mo₆O₁₈NC₆H₄I] (P5). A mixture of 4-iodoaniline (0.219 g, 1 mmol), (n-Bu₄N)₂Mo₆O₁₉ (1.773 g, 1.3 mmol), and DCC (1,3-dicyclohexylcarbodiimide) (0.3094 g, 1.5 mmol) was heated in a 15 mL dry DMSO for 10 h at 70 °C. A colour change to red-orange was seen while the solution heated. After being cooled to room temperature the solution was filtered into a flask containing 200 mL diethyl ether and 50 mL ethanol, removing 1,3-dicyclohexylurea (DCU) and other insoluble materials. An orange precipitate was formed and collected by filtration and then washed with 10 mL ethanol and then ether several times. The resulting solid was recrystallized twice from hot acetonitrile and washed with ethanol and diethyl ether to afford an orange solid (0.86g, 0.549 mmol, 55 %). The final product was dried under vacuum for 24 hours. δ_{H} (500 MHz, CD₃CN) 7.75 (d, $J = 8.5$ Hz, 2H), 6.99 (d, $J = 8.5$ Hz, 2H), 3.09 (t, $J = 8.6$ Hz, 16H) 1.60 (m, 16H), 1.36 (m, 16H), 0.97 (t, $J = 7.4$ Hz, 24H). δ_{C} (125 MHz, CD₃CN). 138.71, 128.43, 59.39, 24.41, 20.42, 13.88. Anal. Calcd (found) % for C₃₈H₇₆N₃O₁₈IMo₆: C, 29.15 (29.09); H, 4.89 (5.01); N, 2.68 (2.70). $m/z = 540$ [C₆H₄NIMo₆O₁₈]²⁻, 440.1 [Mo₆O₁₉]²⁻, 1123.6 [(NBu₄){Mo₆O₁₉}]⁻, 1323.5 [(NBu₄){C₆H₄NIMo₆O₁₈}]¹⁻. FTIR: 2961 (m); 2872 (m); 1560 (vw); 1477 (s); 1376 (m); 1315 (m); 1151 (w); 1106 (vw); 1052 (vw); 1025 (w); 1000 (w); 973 (s); 947 (vs); 878 (m); 829 (m); 770 (vs). UV-Vis (MeCN) λ , nm (ϵ , M⁻¹ cm⁻¹): 205 (48.2×10³); 270 (32×10³); 355 (27×10³).

Synthesis of [(C₄H₉)₄N]₂[Mo₆O₁₈N₂C₁₀H₈] [NBu₄]₂[1]. 4-(1H-pyrrol-1-yl) aniline (0.158 g, 1 mmol), [n-Bu₄N]₂[Mo₆O₁₉] (1.773 g, 1.3 mmol), and DCC (1,3-dicyclohexylcarbodiimide) (0.2886 g, 1.4 mmol) were combined in a dry Schlenk flask under nitrogen and dry DMSO (15 mL) was added. While the solution heated for 10 hours at 65 °C, its colour turned to red. After being cooled to room temperature the red solution was filtered into a flask containing 200 mL dry ether and 50 mL ethanol. The solid was washed with 10 mL ethanol and then ether several times, then the resulting solid recrystallized twice from acetonitrile to yield orange solid (1.2 g, 0.7975 mmol, 80 %). δ_{H} (500 MHz, CD₃CN) 7.49 (d, $J = 8.8$ Hz, 2H), 7.32 (d, $J = 8.8$ Hz, 2H), 7.20 (t, $J = 2.0$ Hz, 2H), 6.31 (t, $J = 2.0$ Hz, 2H), 3.10 (t, $J = 8.6$ Hz, 16H), 1.61 (m, 16H), 1.36 (m, 16H), 0.97 (t, $J = 7.4$ Hz, 24 H). δ_{C} (125 MHz, CD₃CN) 128.50, 120.42, 120.14, 112.18, 59.45, 24.43, 20.42, 13.88. Anal. Calcd (found) % for C₄₂H₈₀N₄O₁₈Mo₆: C, 33.50 (33.59); H, 5.35 (5.29); N, 3.72 (3.65). $m/z = 509.7$ [C₁₀H₈N₂Mo₆O₁₈]²⁻, 439.7 [Mo₆O₁₉]²⁻, 1020 [H{C₁₀H₈N₂Mo₆O₁₈}]¹⁻, 1123.6 [(NBu₄){Mo₆O₁₉}]¹⁻. FTIR: 2962 (m); 2873 (m); 1590 (s); 1505 (s); 1481 (s); 1381 (w); 1324 (s); 1250 (vw); 1178 (m); 1153 (w); 1108 (w); 1062

(s); 1015 (w); 972 (s); 949 (vs); 940 (vs); 914 (s); 880 (m); 843 (s); 771 (vs); 738 (vs). UV-Vis (MeCN) λ (ϵ): 223 (36.3×10^3); 281 (27×10^3); 371 (31.2×10^3).

Synthesis of [(C₄H₉)₄N]₂[Mo₆O₁₈N₂C₁₈H₁₂] [NBu₄]₂[2]. A mixture containing **P4** (0.258 g, 1 mmol), [n-Bu₄N]₂[Mo₆O₁₉] (1.773 g, 1.3 mmol), and DCC (1,3-dicyclohexylcarbodiimide) (0.2886 g, 1.4 mmol) and 15 mL dry DMSO was heated at 70 °C for 10 hours under nitrogen. During the course of the reaction, the solution changed colour to dark-red. After being cooled to room temperature the solution was filtered into a flask containing 200 mL dry ether and 50 mL of ethanol. The solid was washed with ethanol and ether several times, then the resulting solid recrystallized three times from an 50:50; acetonitrile:ethanol mixture to yield orange-red solid (0.8 g, 0.5 mmol, 50 %). δ_{H} (500 MHz, CD₃CN) 7.62 (d, $J = 8.8$ Hz, 2H), 7.55 (d, $J = 8.5$ Hz, 2H), 7.52 (d, $J = 8.8$ Hz, 2H), 7.25 (d, $J = 8.5$ Hz, 2H), 7.23 (t, $J = 2.20$ Hz, 2H), 6.33 (t, $J = 2.20$ Hz, 2H), 3.09 (t, $J = 8.6$ Hz, 16H), 1.61 (m, 16H), 1.36 (m, 16H), 0.97 (t, $J = 7.4$ Hz, 24 H). δ_{C} (125 MHz, CD₃CN) 134.10, 132.67, 127.23, 120.78, 120.06, 112.04, 59.44, 24.41, 20.43, 13.89. Anal. Calcd (found) % for C₅₀H₈₄N₄O₁₈Mo₆: C, 37.41 (37.35); H, 5.27 (5.14); N, 3.49 (3.57). $m/z = 560$ [(C₁₈H₁₂N₂Mo₆O₁₈)²⁻]. FTIR: 2960 (m); 2872 (m); 2210 (vw); 1605 (w); 1584 (w); 1519 (s); 1470 (s); 1378 (m); 1332 (s); 1151 (vw); 1118 (w); 1065 (m); 1017 (vw); 974 (s); 945 (vs); 880 (m); 841 (m); 769 (vs). UV-Vis (MeCN) λ (ϵ): 230 (45.3×10^3); 290 (40.1×10^3); 386 (45.1×10^3).

Synthesis of [(C₄H₉)₄N]₂[C₁₄H₁₀N₂Mo₆O₁₈], [NBu₄]₂[3]. **P5** (790 mg, 0.50 mmol), 4-ethynylaniline (70 mg, 0.6 mmol), Pd(PPh₃)₂Cl₂ (7 mg, 0.01 mmol), CuI (3 mg, 0.02 mmol) and K₂CO₃ (1000 mg, 3.2 mmol) were added to an oven-dried 50 mL round bottom flask containing a magnetic stir bar. The flask was evacuated and backfilled with nitrogen three times. 10 mL anhydrous acetonitrile and 0.5 mL dry triethylamine were then added to the flask with a syringe. After being stirred at room temperature for 0.5 h under nitrogen, the reaction mixture was filtered and the filtrate was then concentrated to about 2 mL before pouring into diethyl ether to afford a red solid. The resulting solid was washed successively with ethanol and ether and then recrystallized twice from (acetonitrile: ethanol) mixture to yield red solid (0.4 g, 0.257 mmol, 51 %). δ_{H} (300 MHz, CD₃CN) 7.46 (d, $J = 8.8$ Hz, 2H), 7.26 (d, $J = 8.5$ Hz, 2H), 7.20 (d, $J = 8.8$ Hz, 2H), 6.63 (d, $J = 8.5$ Hz, 2H), 4.5 (s, 2H), 3.10 (t, $J = 8.63$ Hz, 16H), 1.61 (m, $J = 7.92$ Hz, 16H), 1.37 (m, $J = 7.41$ Hz), 0.97 (t, $J = 7.38$ Hz, 24H). δ_{C} (125 MHz, CD₃CN) 134.01, 132.12, 127.19, 115.14, 59.36, 24.38, 20.42, 13.91. Anal. Calcd (found) % for C₄₆H₈₂N₄O₁₈Mo₆: C, 35.53 (35.41); H, 5.31 (5.26); N, 3.60 (3.49). $m/z = 535$ [C₁₄H₁₀N₂Mo₆O₁₈]²⁻, 439.6 [Mo₆O₁₉]²⁻, 1123.6 [(NBu₄){Mo₆O₁₉}]¹⁻, 1311.69 [(NBu₄){C₁₄H₁₀N₂Mo₆O₁₈}]¹⁻. FTIR: 3362 (w); 2960 (m); 2872 (m); 2201 (m); 1619 (m); 1605 (m); 1582 (m); 1515 (m); 1481 (m); 1331 (m); 1300 (w); 1179 (w); 1135 (w); 1064 (vw); 1029 (vw); 974 (m); 946 (vs); 840 (m); 773 (vs). UV-Vis (MeCN) λ (ϵ): 226 (44.4×10^3); 281 (39.2×10^3); 403 (35.8×10^3).

X-ray Crystallographic Details

Sample Growth, Data Collection and Refinement. Crystals of [NBu₄]₂[1], [NBu₄]₂[2], and [NBu₄]₂[3] were obtained by room temperature diffusion of diethyl ether vapor into acetonitrile. Data were collected on Oxford Diffraction XCalibur 3 diffractometer, or a Rigaku AFC 12 goniometer equipped with an enhanced sensitivity (HG) Saturn724+ detector and FR-E+ SuperBright molybdenum rotating anode generator with HF Varimax optics (100 μm focus). Data reduction, cell refinement and absorption correction was carried out using Agilent Technologies CrysAlisPro⁹ or Rigaku CrystalClear-SM Expert software,¹⁰ and solved using SHELXS-2014¹¹ via WinGX.¹² Refinement was achieved by full-matrix least-squares on all F_0^2 data using SHELXL-2014¹³ and molecular graphics were prepared using ORTEP-3.¹⁴ Both [NBu₄]₂[2] and [NBu₄]₂[3] showed

disorder requiring the use of restraints on thermal parameters and certain bond distances. Full crystallographic data and refinement details are presented in Table S1. Note that while the Flack parameter for [NBu₄]₂[**3**] suggests this structure may be better in a centrosymmetric group, refinement in the alternative *Pbca* results in a significantly higher *R*-factor (*R*₁ = 13%). In [NBu₄]₂[**1**] and [NBu₄]₂[**2**], the asymmetric unit contains the complete molecular anion and both cations, while in [NBu₄]₂[**3**] there are two crystallographically independent anions, and four crystallographically independent [NBu₄]⁺ cations. See Figure S1 to S3.

Structures and Selected Bond Lengths. ORTEP representations of the asymmetric units of the three structures are displayed below in Figures S1a to S3a, along with crystal packing diagrams. Selected bond lengths and angles in the anions are collected in Table S2. In all three structures, the Mo-N-C bond angle is closer to 180° than 120°, indicating significant Mo-N triple bond character. The compounds also show the typical imido-Lindqvist pattern of a shortened bond length from the imido-Mo (Mo^{im}) to the central oxygen (O^c), lengthened equatorial bond lengths from Mo^{im} to the oxygens bridging to the belt Mo positions (Mo^b), and a lengthened axial bond length from the *trans*-Mo (Mo^l) to O^c (see references 17a and 20, main paper). There is, however, no consistent pattern in the terminal Mo=O distances which are typically in the range of 1.65 to 1.70 Å. While [NBu₄]₂[**2**] and [NBu₄]₂[**3**] are solved in non-centrosymmetric groups, the packing of the POM chromophores is not polar, so these are not bulk NLO materials. This is evident from the packing diagrams in (Figures S2b and S3b) which show that the dipoles of different chromophores oppose each other. The only significant intermolecular interactions between the chromophores are C-H...O contacts between aromatic groups and molybdate groups (present in all structures: C...O distances 3.153 to 3.461 Å; H...O 2.392 to 2.684 Å), and hydrogen bonds between the aniline moieties in [NBu₄]₂[**3**] and molybdate (N...O 2.981 Å to 3.000 Å; H...O 2.093 Å to 2.152 Å)

Table S1. Crystallographic Data and Refinement Details for [NBu₄]₂[**1**], [NBu₄]₂[**2**] and [NBu₄]₂[**3**]

| | [NBu ₄] ₂ [1] | [NBu ₄] ₂ [2] | [NBu ₄] ₂ [3] |
|--|--|--|--|
| Formula | C ₄₂ H ₈₀ Mo ₆ N ₄ O ₁₈ | C ₅₀ H ₈₄ Mo ₆ N ₄ O ₁₈ | C ₄₆ H ₈₂ Mo ₆ N ₄ O ₁₈ |
| <i>M</i> | 1504.74 | 1604.85 | 1554.79 |
| cryst syst | Monoclinic | Orthorhombic | Orthorhombic |
| space group | <i>P</i> 2 ₁ / <i>n</i> | <i>P</i> 2 ₁ 2 ₁ 2 ₁ | <i>P</i> 2 ₁ 2 ₁ 2 ₁ |
| <i>a</i> /Å | 11.6395(2) | 17.559(1) | 15.927(1) |
| <i>b</i> /Å | 33.6792(5) | 17.783(1) | 24.542(2) |
| <i>c</i> /Å | 14.0382(2) | 19.608(1) | 29.984(2) |
| <i>α</i> /deg | 90 | 90 | 90 |
| <i>β</i> /deg | 91.577(1) | 90 | 90 |
| <i>γ</i> /deg | 90 | 90 | 90 |
| <i>U</i> /Å ³ | 5501.0(2) | 6122.7(7) | 11720(2) |
| <i>Z</i> | 4 | 4 | 8 |
| <i>T</i> /K | 140(2) | 100(2) | 100(2) |
| <i>μ</i> /mm ⁻¹ | 1.397 | 1.260 | 1.314 |
| Cryst. size/mm | 0.32 x 0.25 x 0.07 | 0.12 x 0.06 x 0.01 | 0.190 x 0.180 x 0.030 |
| Cryst. description | Orange plate | Orange blade | Orange |
| No. reflns collected | 122706 | 42376 | 153015 |
| No. of indep. reflns (<i>R</i> _{int}) | 18893 [R(int) = 0.0572] | 14052 [R(int) = 0.0827] | 26880 [R(int) = 0.0742] |
| <i>θ</i> _{max} /deg (completeness) | 99.8% | 99.7 % | 99.8 % |
| Reflections with <i>I</i> > 2σ(<i>I</i>) | 15094 | 5819 | 6256 |
| Goodness-of-fit on <i>F</i> ² | 1.191 | 0.914 | 0.985 |
| Flack parameter | N/A | 0.01(4) | 0.61(5) ^a |
| final <i>R</i> ₁ , <i>wR</i> ₂ [<i>I</i> > 2σ(<i>I</i>)] ^a | <i>R</i> ₁ = 0.0566, <i>wR</i> ₂ = 0.0888 | <i>R</i> ₁ = 0.0702, <i>wR</i> ₂ = 0.1543 | <i>R</i> ₁ = 0.0533, <i>wR</i> ₂ = 0.1442 |

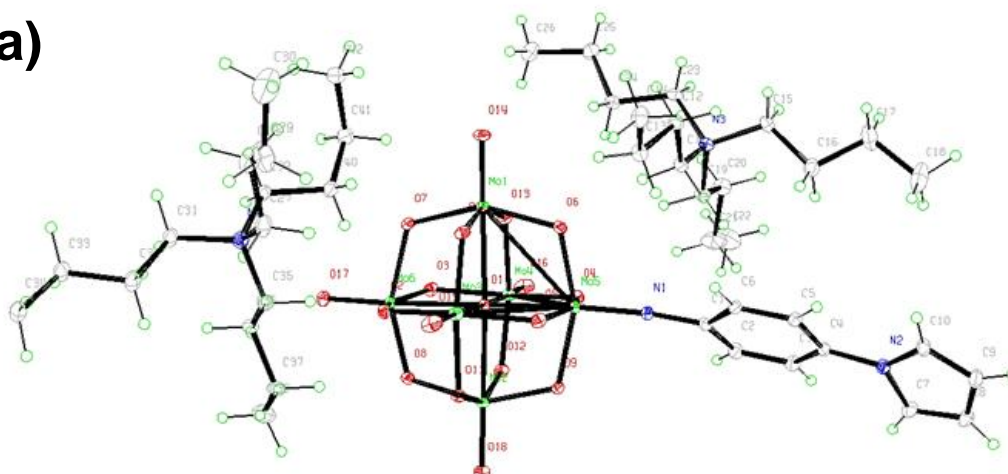
| | | | |
|---------------------------------|---------------------------|---------------------------|---------------------------|
| (all data) | R1 = 0.0758, wR2 = 0.0948 | R1 = 0.1716, wR2 = 0.1956 | R1 = 0.0558, wR2 = 0.1466 |
| Peak and hole/e Å ⁻³ | 1.707 and -1.884 | 0.793 and -0.385 | 1.571 and -1.040 |

^aAlthough ADDSYMM finds additional symmetry elements, refining in the alternative, centrosymmetric group of *Pbca* results in significantly worse R_1 and wR_2 .

Table S2 Selected bond lengths (Å) and angles (°) in the anions of compounds **1** to **3**. Mo^{im} – imido bearing Mo; Mo^b belt Mo; Mo^t, *trans*-Mo; O^c, central O; O^b, bridging O.

| | 1 | 2 | 3 |
|--|----------|-----------|----------|
| C-N-Mo ^{im} | 173.3(3) | 172.7(11) | 176.1(7) |
| N-Mo ^{im} | 1.738(3) | 1.734(11) | 1.738(7) |
| Mo ^{im} -O ^c | 2.206(2) | 2.234(7) | 2.196(5) |
| Mo ^{im} -O ^b (average) | 1.951(3) | 1.946(8) | 1.947(6) |
| Mo ^b -O ^c (average) | 2.337(5) | 2.325(8) | 2.340(5) |
| Mo ^b -O ^b (average) | 1.921(3) | 1.907(9) | 1.928(7) |
| Mo ^t -O ^c | 2.361(3) | 2.341(8) | 2.353(5) |
| Mo ^t -O ^b (average) | 1.920(3) | 1.941(9) | 1.918(7) |

(a)



(b)

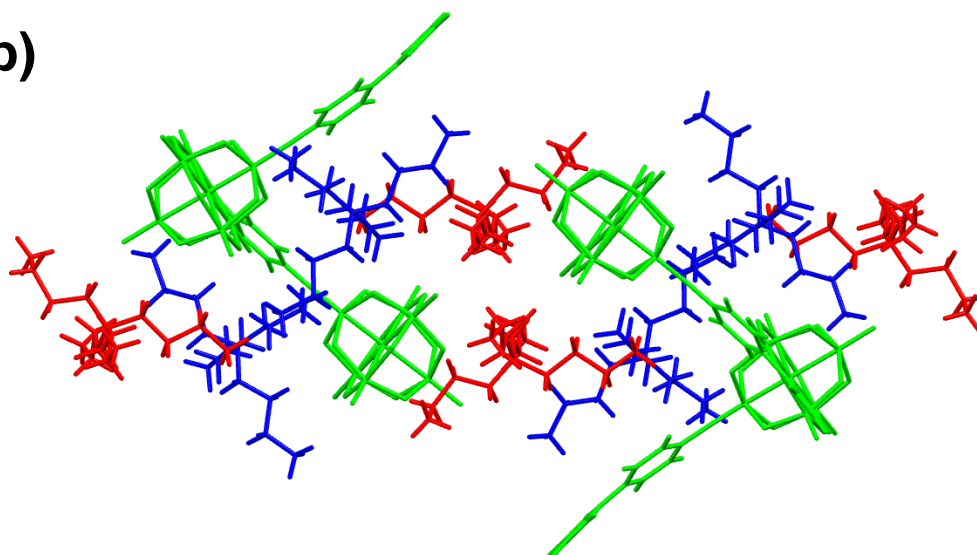


Figure S1 (a) ORTEP representation of the asymmetric unit in $[\text{NBu}_4]_2[\mathbf{1}]$. Thermal ellipsoids are at the 30% probability level. Color scheme: Mo is green; O, red; C, gray; N, blue; H atoms are represented by green circles of arbitrary radii. (b) Crystal packing diagram viewed along the crystallographic c -axis, for clarity colours are by symmetry equivalence with $[\mathbf{1}]^{2-}$ in green, and $[\text{NBu}_4]^+$ in blue/red.

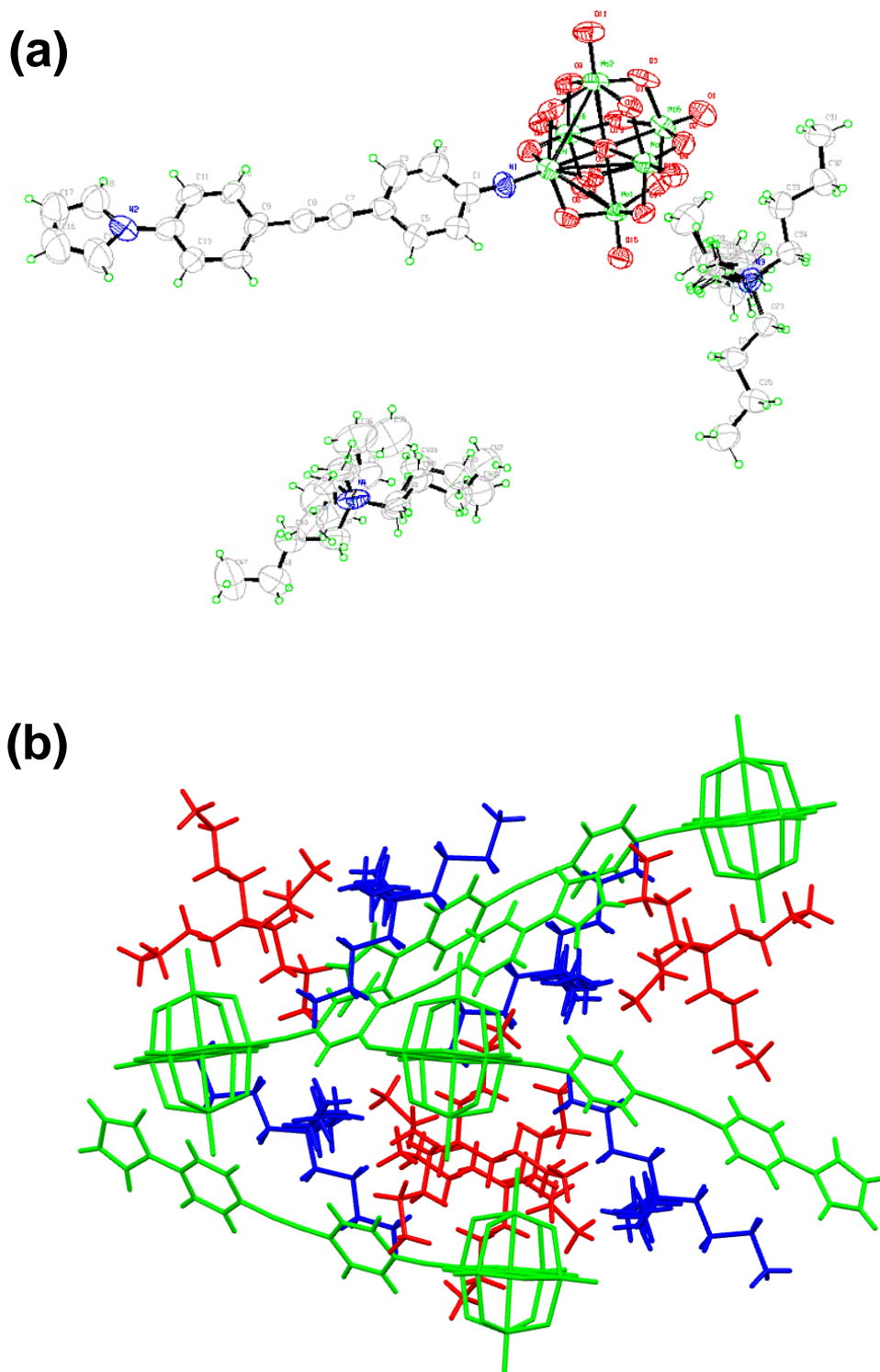


Figure S2 (a) ORTEP representation of the asymmetric unit in $[\text{NBu}_4]_2[\mathbf{2}]$. Thermal ellipsoids are at the 30% probability level. Color scheme as Figure S1. (b) Crystal packing diagram viewed along the

crystallographic *b*-axis, for clarity colours are by symmetry equivalence with $[2]^{2-}$ in green, and $[\text{NBu}_4]^+$ in blue/red, and disordered atoms are omitted.

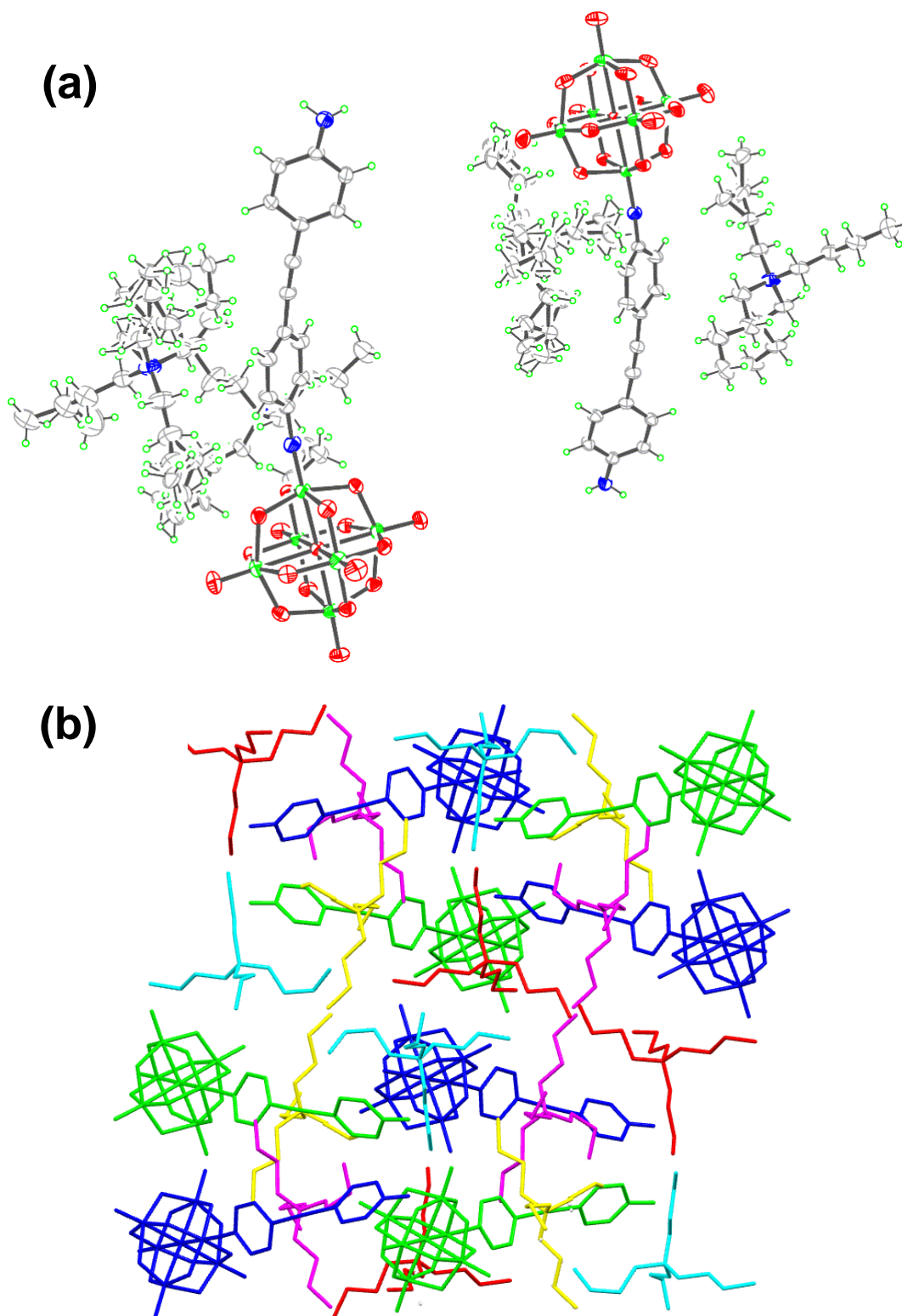


Figure S3 (a) ORTEP representation of the asymmetric unit in $[\text{NBu}_4]_2[\mathbf{3}]$. Thermal ellipsoids are at the 30% probability level. Color scheme: as Figure S1, atom labels omitted for clarity. (b) Crystal packing diagram viewed along the crystallographic *a*-axis, for clarity colours are by symmetry

equivalence with [3]²⁻ in green/royal blue, and [NBu₄]⁺ in red/yellow/purple/light blue, disordered atoms are omitted.

Hyper-Rayleigh Scattering

General details of the hyper-Rayleigh scattering (HRS) experiment have been discussed elsewhere,¹⁵ and the experimental procedure and data analysis protocol used for the fs measurements used in this study were as previously described.¹⁶ Measurements were carried out using dilute (*ca.* 10⁻⁵ M) filtered (Millipore, 0.45 μm) acetonitrile solutions, such that self-absorption of the SHG signal was negligible, verified by the linear relation between signal and concentration. Crystal violet was used as an external reference ($\beta_{xxx,800} = 338 \times 10^{-30}$ esu in methanol,^{16a} corrected for local field factors at optical frequencies). All 800 nm measurements were performed by using the 800 nm fundamental of a regenerative mode-locked Ti³⁺:sapphire laser (Spectra Physics, model Tsunami®, 100 fs pulses, 2 W, 80 MHz). An absence of demodulation for compounds **1** and **3**, i.e. constant values of β versus frequency, showed that no multiphoton fluorescence contributions to the HRS signals were present at 400 nm. This situation may indicate: (i) a lack of fluorescence, (ii) spectral filtering out of fluorescence, or (iii) the fluorescence lifetime is too short for its demodulation to be observed within the bandwidth of the instrument. The fluorescence of **2** has been corrected for by demodulation fitting to provide a fluorescence free value of β . The reported β values are the averages taken from measurements at different amplitude modulation frequencies. Measurements at 1064 nm were carried out in acetonitrile, using a Spectra-Physics InSight® DS+ laser (1W average power, sub-100 fs pulses, 80 MHz). In this setup, the collection optics are coupled to a spectrograph (model Bruker 500is/sm), together with an EMCCD camera (Andor Solis model iXon Ultra 897). Correction for multiphoton induced fluorescence was done by subtracting the broad MPF background signal from the narrow HRS peak (FWHM ± 9 nm). The higher accuracy of this setup enables us to use the solvent as an internal reference (acetonitrile, $\beta_{HRS,1064} = 0.258 \times 10^{-30}$ esu; $\beta_{zzz,1064} = 0.623 \times 10^{-30}$ esu).¹⁷

Electron Number Adjusted β : Organoimido-POMs vs Comparable Organic Systems

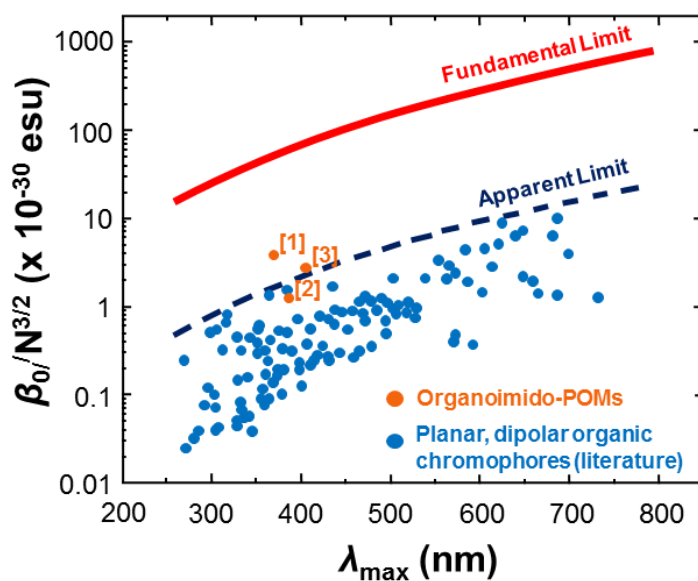


Fig. S4 Data showing electron number adjusted β values ($\beta_0/N^{3/2}$ where $N = \pi$ conjugated electrons in bridge) plotted against the wavelength of maximum absorption, λ_{max} for organoimido-POM anions **1**

to **3**, and planar, dipolar organic chromophores from the literature. [**1**]²⁻ and [**3**]²⁻ both exceed expected performance limits for comparable organic systems. Limits and literature data taken from reference 23a of the main paper.

References

1. W. L. F. Armarego and C. L. L. Chai, *Purification of laboratory chemicals*; 6th ed.; Elsevier/Butterworth-Heinemann: Amsterdam; Boston, 2009.
2. W. G. Klemperer, *Inorg. Synth.* 1990, **27**, 71.
3. H.-J. Deng, Y.-J. Fang, G.-W. Chen, M.-C. Liu, H.-Y. Wu and J.-X. Chen, *Appl. Organometallic Chem.* 2012, **26**, 164.
4. I. Bar-Nahum, K. V. Narasimhulu, L. Weiner and R. Neumann, *Inorg Chem.* 2005, **44**, 4900.
5. S. K. Ibrahim, Ph.D Thesis, University of Sussex, 1992.
6. L. Xu, M. Lu, B. Xu, Y. Wei, Z. Peng and D. R. Powell, *Angew. Chem. Int. Ed.* 2002, **41**, 4129.
7. M. B. Gawande and P. S. Branco, *Green. Chem.* 2011, **13**, 3355.
8. N. C.-K. Elming, *Acta. Chim. Scand.* 1952, **6**, 867.
9. *CrysAlisPro* (Version 1.171.36.21), Agilent Technologies, Inc.; Santa Clara: CA, United States, 2012.
10. *CrystalClear-SM Expert* (Version 3.1 b27), Rigaku Corporation; Tokyo: Japan, 2013.
11. G. M. Sheldrick, *SHELXS-2014*, Programs for Crystal Structure Analysis (Release 2014-7); University of Göttingen: Göttingen, Germany, 2014.
12. L. J. Farrugia, *J. Appl. Cryst.* 1999, **32**, 837.
13. G. M. Sheldrick, *SHELXL-2014*, Programs for Crystal Structure Analysis (Release 2014-7); University of Göttingen: Göttingen, Germany, 2014.
14. L. J. Farrugia, *J. Appl. Cryst.* 1997, **30**, 565.
15. (a) K. Clays and A. Persoons, *Phys. Rev. Lett.* 1991, **66**, 2980. (b) K. Clays and A. Persoons, *Rev. Sci. Instrum.* 1992, **63**, 3285. (c) E. Hendrickx, K. Clays and A. Persoons, *Acc. Chem. Res.* 1998, **31**, 675.
16. (a) G. Olbrechts, R. Strobbe, K. Clays and A. Persoons, *Rev. Sci. Instrum.* 1998, **69**, 2233. (b) G. Olbrechts, K. Wostyn, K. Clays and A. Persoons, *Optics Lett.* 1999, **24**, 403. (c) K. Clays, K. Wostyn, G. Olbrechts, A. Persoons, A. Watanabe, K. Nogi, X.-M. Duan, S. Okada, H. Oikawa, H. Nakanishi, H. Vogel, D. Beljonne and J.-L. Brédas, *J. Opt. Soc. Am. B* 2000, **17**, 256. (d) E. Franz, E. C. Harper,

B. J. Coe, P. Zahradnik, K. Clays and I. Asselberghs, *Proc. SPIE–Int. Soc. Opt. Eng.* 2008, **6999**, 699923-1–699923-11.

17. J. Campo, F. Desmet, W. Wenseleers and E. Goovaerts, *Opt. Express* 2009, **17**, 4587.